ACS APPLIED MATERIALS & INTERFACES

www.acsami.org Research Article

Graphene Oxide and Metal–Organic Framework-Based Breathable Barrier Membranes for Toxic Vapors

Yufeng Song, Cheng Peng, Zafar Iqbal, Kamalesh K. Sirkar,* Gregory W. Peterson, John J. Mahle, and James H. Buchanan

Cite This: *ACS Appl. Mater. Interfaces* 2022, 14, 31321–31331 Read Online

ACCESS | Metrics & More | Article Recommendations | Supporting Information

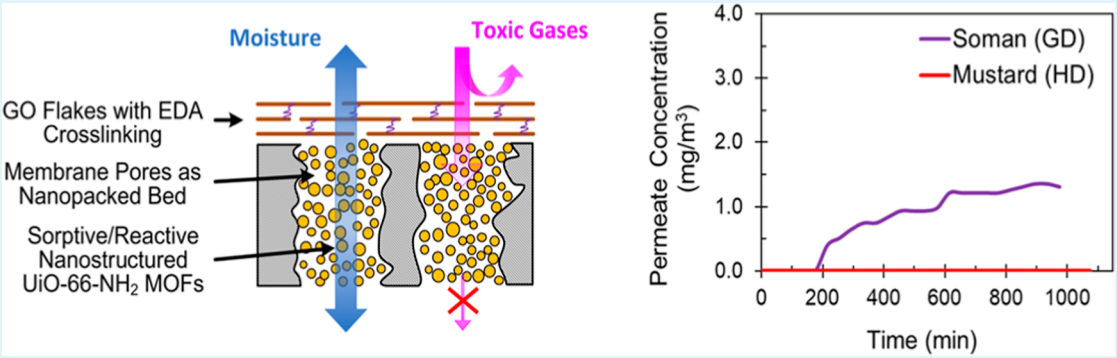

ABSTRACT: Garments protective against chemical warfare agents (CWAs) or accidently released toxic chemicals must block the transport of toxic gases/vapors for a substantial time and allow moisture transport for breathability. These demands are challenging: either the barriers block CWAs effectively but have poor breathability or barriers have excellent breathability but cannot block CWAs well. Existing protective garments employ large amounts of active carbon, making them quite heavy. Metal–organic framework (MOF)-based adsorbents are being investigated as sorbents for CWAs. Breathable laminate of graphene oxide (GO) flakes supported on a porous membrane reduces permeation rates of CWA simulants substantially. We developed a multilayered membrane-based flexible barrier: GO laminate-based membrane over a MOF nanocrystal-filled expanded polytetrafluorethylene (ePTFE) membrane having submicrometer pores. The GO laminate-based layer developed a steady breakthrough concentration level almost 2 orders of magnitude below the usual breakthrough level. This highly reduced level of CWA was blocked by the MOF nanocrystal-filled membrane substrate layer over a highly extended period. We demonstrated the blocking of CWAs, mustard (HD), soman (GD), a sarin simulant [dimethyl methyl phosphonate (DMMP)], and ammonia for an extended period while the moisture transmission rate was substantial. The times for complete blockage of ammonia, HD, GD, and DMMP were 2750 min, 1075 min, 176 min, and 7 days, respectively. This remarkable performance resulted from a very low steady-state penetrant permeation through GO-laminate membrane and substantial penetrant sorption by MOF nanocrystals; furthermore, both layers show high moisture vapor transmission.

KEYWORDS: *multilayer barrier structure, chemical warfare agents, breathable fabric, graphene oxide laminate membrane, metal–organic framework, nano-scale packed bed*

INTRODUCTION

Garments acting as protective fabric/barrier are employed to protect personnel from exposure to chemical warfare agents (CWAs) and toxic gases and vapors accidently released in manufacturing facilities. Such structures/garments must be breathable with sufficient moisture transmission capability and yet block completely transmission of harmful gases/vapors for extended periods. These garments are heavy because a large amount of porous sorbents, for example, active carbons, are employed for total protection from chemical and biological threat including CWAs. Typical CWA simulants studied are dimethyl methyl phosphonate (DMMP) (a sarin-simulant) and 2-chloroethyl ethyl sulfide (CEES) (a simulant for sulfur mustard).

A variety of materials, material structures, and membranes have been studied vis-a-vis their barrier properties[1,2] for blocking toxic gases and vapors including breathability[3] (see

Received: May 6, 2022
Accepted: June 21, 2022
Published: June 30, 2022

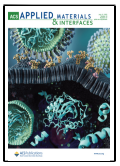

https://doi.org/10.1021/acsami.2c07989
ACS Appl. Mater. Interfaces 2022, 14, 31321–31331

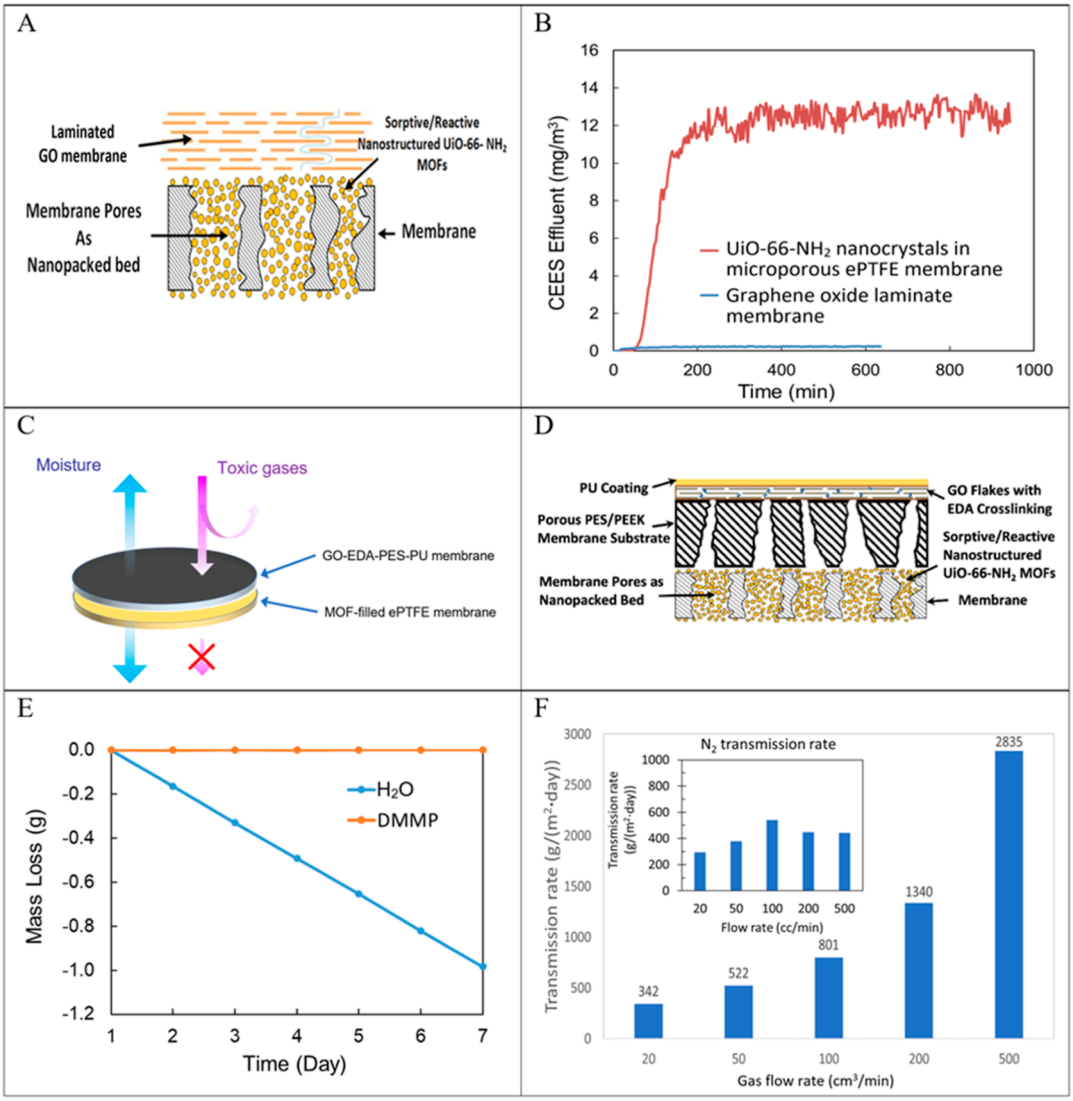

Figure 1. GO-MOF multilayer membrane and illustrative 25 °C performances for DMMP blockage and moisture removal. (A) Schematic of blockage concept: a GO laminate membrane[23,32,33] on top of a MOF-filled porous membrane. (B) CEES permeation rate through individual barriers: GO laminate membrane;[22] UiO-66-NH_2 MOF-filled porous ePTFE membrane.[21] (C) Functional schematic of a moisture-permeable multilayer barrier against toxic gases and vapors. (D) Details of the actual multilayer structure-schematic. (E) Upright cup method results in separate experiments for water vapor and sarin simulant DMMP for GO-MOF multilayer membrane for 7 days. (F) Moisture transmission rates obtained in the DMPC for GO-MOF multilayer membrane. Membrane dimensions in Figure 1E,F are 1.8 and 3.0 cm, respectively. The method for fabrication of the GO layer is illustrated in Figure S4.

earlier literature[4−7]). Recently, there has been an increasing focus on metal−organic frameworks (MOFs) for removing toxic gases by adsorption and destruction. Independent sorption and breakthrough studies of NH_3 and CNCl through a packed bed of pellets of MOF UiO-66-NH_2 were implemented[8] in a micro-breakthrough and regular test-tube packed beds setup under dry and humid conditions. Ammonia sorption and breakthrough studies for various functionalized variations of Zr-based MOF UiO-66 [UiO-66-OH, UiO-66-$(OH)_2$, UiO-66-NO_2, UiO-66-NH_2, UiO-66-SO_3H, and UiO-66-$(COOH)_2$] in a packed bed were carried out[9] with dry and humid air. High NH_3 capture/storage capacity was demonstrated by modifying the surface of pores in covalent organic networks (CONs).[10,11]

Other formats for using MOFs in barriers/suits have been studied for protection against CWAs. Electrospun nanofibers of polystyrene containing MOF UiO-66-NH_2 were studied to remove Cl_2 and the nerve agent soman.[12] Layers of pure MOF as a membrane or mixed matrix membranes (MMMs) having MOFs dispersed in a polymer have been studied for a variety of separations.[13−16] Such membranes are usually thin and prepared for steady-state gas separations. They cannot completely block a selected gas/vapor species. This is true even when a gas separation membrane has a very high selectivity of 15,000−18,000.[17] A much thicker membrane (20 mil) with a high loading (50%) of the MOF HKUST-1 in an elastomeric triblock copolymer[18] had a high permeation lag time: the breakthrough time for CEES feed concentration was high, ∼4000 min. The moisture vapor transmission rate (MVTR) was however low ∼192 g/m^2 day (required minimum ∼2000 g/m^2 day[19]). Extended duration CWA blockage is needed along with high MVTR values.

An alternative to the MMM concept[18] employs a membrane-based strategy involving a serial membrane

https://doi.org/10.1021/acsami.2c07989
ACS Appl. Mater. Interfaces 2022, 14, 31321−31331

structure using carbon nanotubes (CNTs). Using a highly breathable CNT-membrane providing an effective barrier against biological agents as a base,[19] a layer of polymer chains was grown on the top surface of the CNTs. The polymer chains reversibly collapsed in contact with a CWA threat, thus temporarily shutting CNT pore mouths and drastically reducing the permeation rate of the nerve agent simulant across the membrane.[20] The nerve agent simulant was diethyl chlorophosphate (DCP); experiments showed that DCP permeation was restricted to ≈1% of the chemical challenge.

We recently developed[21] a 79 μm thick, porous flat membrane-supported nano-packed bed of MOF UiO-66-NH_2 which needed ∼200−300 min for ammonia to appear in the dead-end mode on the other side of the membrane; the MVTR values were ∼5000 g/m^2 day. We also investigated a graphene oxide (GO)-based barrier membrane possessing a high MVTR to drastically reduce the permeation rate of CWAs.[22] Under appropriate conditions, graphene (GR)-based as well as GO-based membranes can shut off gas permeation except for moisture vapor and traces of He.[23] Multilayered GO platelet-based membranes at zero relative humidity (RH) are essentially impermeable to small gases but allow H_2O vapor to go through GO nano-capillaries between GR sheets via water monolayers; this structure prevents other gases/vapors from flowing especially under reduced humidity. Our studies[22] showed that multilayered GO membrane blocked DMMP vapor for 15 days. There are several studies which illustrate and illuminate the extraordinary barrier properties of GO-based membranes.[24−27]

This study explores the breakthrough and permeation behavior of toxic gases and vapors through a novel composite structure: a GO-based multilayered composite membrane at the top exposed to the toxic gas mixture and backed up by a membrane-supported MOF, UiO-66-NH_2, forming a nano-packed bed at the bottom/permeate side. Earlier fabrication of a porous expanded polytetrafluoroethylene (ePTFE) membrane-supported nanopacked bed of MOF nanocrystals via solvothermal synthesis[21] involved a lengthy solvent exchange procedure to incorporate 80:20 ratio of the DMF−methanol solvent mixture in the pores of the PTFE membrane because DMF does not wet the pores of the hydrophobic ePTFE membrane but is needed for MOF synthesis.[28,29] A much more facile synthesis of such a structure was pursued here. The CWAs/vapors/gases whose blockages/permeations have been studied include DMMP (a sarin-simulant), sulfur mustard (HD), nerve agent soman (GD), NH_3, and N_2. Two sample sizes were prepared for various experiments: 4.7 and 9.0 cm. We report here a complete shut-off of CWAs, HD and GD, a CWA simulant, DMMP, and NH_3 for an extended period.

RESULTS AND DISCUSSION

We illustrate a conceptual schematic of the multilayer structure needed for the core concept in Figure 1A. The top layer built of a multi-layered GO platelet-based membrane is essentially impermeable to small gases at zero RH but allows H_2O vapor to go through GO nano-capillaries between closely spaced graphene (GR) sheets via water monolayers.[23] Under humid conditions, water vapor shows high selectivity over various small gases/vapors, for example, N_2, ethane.[22] Earlier studies by others[24,25] showed considerable selectivity for water vapor over environmental toxicants, for example, benzene, hexane, chloroform, etc. We demonstrated complete blockage of toluene.[22] This top GO-layer is conceptually placed over a nanoporous membrane whose pores are filled with UiO-66-NH_2 MOF nanocrystals.

Figure 1B illustrates the individual permeation behavior of each individual part of this hypothetical structure. When exposed to a feed concentration of 300 mg/m^3 of CEES in air, the MOF-containing layer blocked CEES transmission completely for 46 min. Then, slowly CEES appeared and completely broke through at around 150 min;[21] the breakthrough concentration was 12 mg/m^3 due to dilution by sweep air on the other side of the membrane. When the GO-layer was exposed to the same 300 mg/m^3 of CEES containing air stream, there was complete blockage for 16 min only. However, CEES then slowly appeared and maintained a steady rate of permeation for a constant breakthrough concentration of around 0.25 mg/m^3 (corresponding to a steady 97.2% rejection with respect to a breakthrough concentration of 12 mg/m^3) for 600 min when the experiment was stopped.[22] This very low value of 0.25 mg/m^3 is to be contrasted with the high breakthrough concentration of 12 mg/m^3 in the case of the MOF barrier. These numbers suggest that the very strong reduction of the CEES permeation rate through the top GO layer will provide such a low level of challenge for the MOF-containing layer as to prevent a breakthrough for a considerable length of time. These two layers have altogether different functions from CWA sorption/transport perspectives and can together provide a platform for blocking other vapors/gases by selecting, for example, appropriate MOFs.

Figure 1C shows an illustrative schematic of such a layered structure that blocks toxic penetrants but allows moisture to go through. Figure 1D provides details of such a layered structure. The top part contains a GO laminate-based membrane crosslinked with ethylene diamine (EDA); it is supported at the bottom on a porous polyethersulfone membrane via $\pi-\pi$ bonding[30] and coated at the top by a thin polyurethane (PU) coating as an anti-scratching layer. The bottom part of the structure is a 79 μm thick, porous ePTFE membrane whose sub-micrometer pores/interfibrillar space are filled with nanocrystals and sub-micrometer size crystals of MOF, UiO-66-NH_2, grown in situ by solvothermal synthesis.[21] The performance of such a multilayer structure as a vapor/gas barrier is illustrated next for moisture and sarin-simulant DMMP in Figure 1E,F. Using the upright cup test method (Figure S1), Figure 1E plots the data of mass loss versus time in days obtained in separate experiments for moisture and DMMP. For 7 days, no loss was recorded for DMMP, but there was a significant and continuing loss of water. The data for mass loss are available in Table S1 along with the water vapor flux.

The corresponding values for only the GO part of the membrane are provided in Figure S2 which also illustrates the considerable effect of the boundary layer resistance in the upright cup method. To determine the true moisture vapor permeation rate, we used the dynamic moisture permeation cell (DMPC)[31] (Figure S3) to eliminate the boundary layer resistance by increasing the feed and He sweep gas flow rate. The measured MVTR (Figure 1F) exceeds the required minimum of 1500−2000 g/m^2 day.[19,22] The insert in Figure 1F shows that the feed and sweep gas flow rate variation does not influence the permeance of the much less permeable gas, N_2.[22] Permeances of the following gas species, N_2, ethane, ethylene, He, as well as water vapor measured in the DMPC through such a multi-layered structure and reported in Table

https://doi.org/10.1021/acsami.2c07989
ACS Appl. Mater. Interfaces 2022, 14, 31321−31331

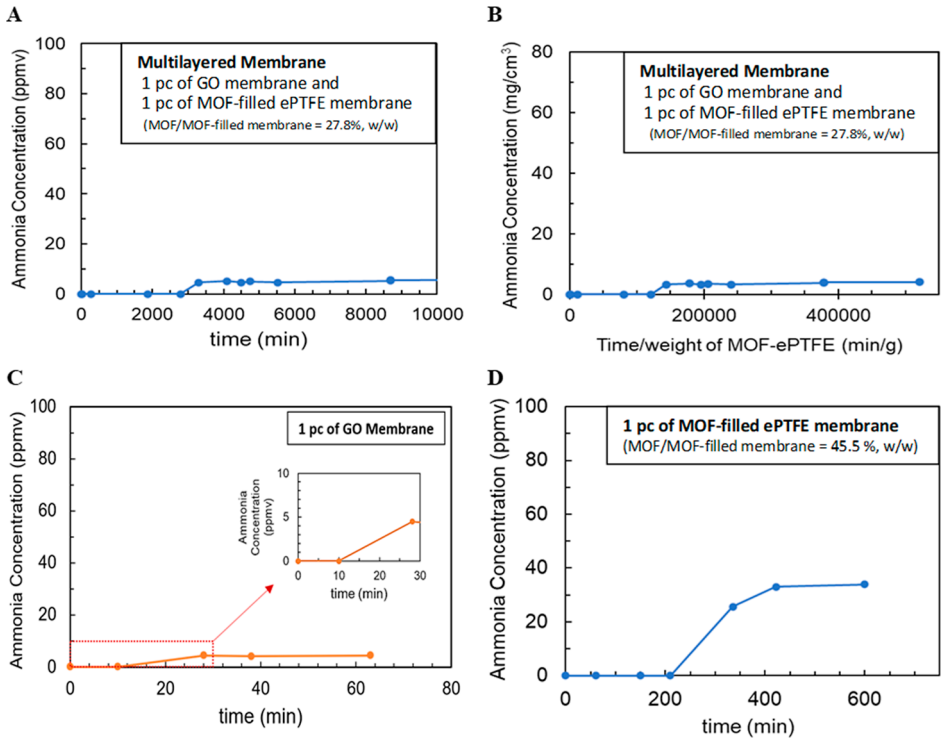

Figure 2. Time dependence of NH_3 blockage from a 100 ppmv NH_3-containing dry N_2 feed gas stream[1] by the multilayer GO-MOF membrane (Figure 1D) and two individual membrane parts. (A) Multilayer membrane: GO membrane (47 mm diameter) exposed to feed N_2 stream supported by the MOF-filled membrane at the bottom. (B) Alternative plot illustrates NH_3 blockage versus time/(weight of MOF and ePTFE membrane in the multilayer membrane). (C) NH_3 blocking behavior by GO layer only. (D) NH_3 blocking behavior by the MOF-filled ePTFE membrane only. [1]N_2 feed gas stream flowing at 10 cm^3/min at 25 °C in the DMPC.

S2 show how high the water vapor permeance is compared to those of others. In general, the larger is the kinetic diameter of the gas, the smaller is its permeance through GO laminate membrane.[22]

The permeances reported in Table S2 are pure gas permeances for He, and N_2 so that ideal selectivity can be obtained by dividing individual permeances. From these values, we find ideal selectivity of H_2O/He, H_2O/N_2, and He/N_2 systems to be, respectively, 6.9, 216, and 31.3. However, the data for ethylene and ethane were obtained from a 50−50 feed mixture; the corresponding selectivity for H_2O/C_2H_4, H_2O/C_2H_6, and C_2H_4/C_2H_6 systems are 1317, 1460, and 1.1. The results for these four gases show how permeable the GO-MOF membrane is to water vapor. It is useful to recall here that GO flakes dispersed in a polymer matrix[34] or reduced GO (rGO) flakes dispersed in an organo-silica network,[35] creating a MMM display considerable selectivity for CO_2 over N_2. In polysulfone (PsF) hollow fibers, only 0.25% GO in PsF enhanced mixed gas selectivity for CO_2/N_2 by 201%.[34] In a 1:1 r-GO/silica membrane on a support, the selectivities for H_2/CH_4 and CO_2/CH_4 were found to be 223 and 55, respectively.[35] By intercalating Fe ions in mildly reduced GO (rGO)-based gas separation membranes,[36] an excellent N_2/CO_2 selectivity of ∼97 was obtained at 110 mbar. After introducing Mg^{2+} ions within GO channels,[37] the CO_2/N_2 separation factor of the GO membrane is remarkably increased from 4 to 48.8 with CO_2.

The performances of our multilayer structure shown in Figure 1D and its component parts are illustrated in Figure 2 when exposed to a 100 ppmv NH_3-containing N_2 gas stream as feed; the diffusive permeate is picked up by a sweep N_2 gas stream in the DMPC. The base membrane size for the GO part was 47 mm. The permeate NH_3 concentration under feed breakthrough conditions is naturally lower than the feed concentration level of 100 ppmv NH_3 due to sweep N_2 gas-based dilution. Figure 2A shows that when a multilayered GO-MOF membrane of Figure 1D is used, ammonia is blocked for 2790 min; then, it appears at an approximately constant level of around 5.3 ppmv after a ramp up. Figure 2B reports such a result in an alternate fashion by plotting ammonia concentration on the permeate side against the ratio of time per unit weight of ePTFE plus the MOF in min/g.

The breakthrough performance of the GO part of the multilayer membrane is shown in Figure 2C. This structure completely blocks NH_3 for only 10 min; however, its characteristic behavior reduces the steady leakage rate to a very low level of 4.4 ppmv. On the other hand, the MOF-filled ePTFE membrane part of the multilayer structure blocks ammonia for 210 min (Figure 2D); then, ammonia appears in the sweep gas and its concentration there rises slowly and steadily to 34 ppmv. It is now clear that the very low value of the steady leakage rate through the top GO part of the structure allows the MOF-filled bottom supporting membrane layer to hold back ammonia breakthrough to a high value of 2790 min.

The earlier technique of solvothermal synthesis of UiO-66-NH_2 MOF nanoparticles in the sub-micrometer ePTFE membrane pores/interfibrillar space[21] involved an extended 6-step solvent-exchange process to incorporate 80% DMF−20% methanol in the membrane pores which are not spontaneously wetted by the highly polar aprotic DMF-based solvents. The reactants were then introduced into the liquid in

https://doi.org/10.1021/acsami.2c07989
ACS Appl. Mater. Interfaces 2022, 14, 31321−31331

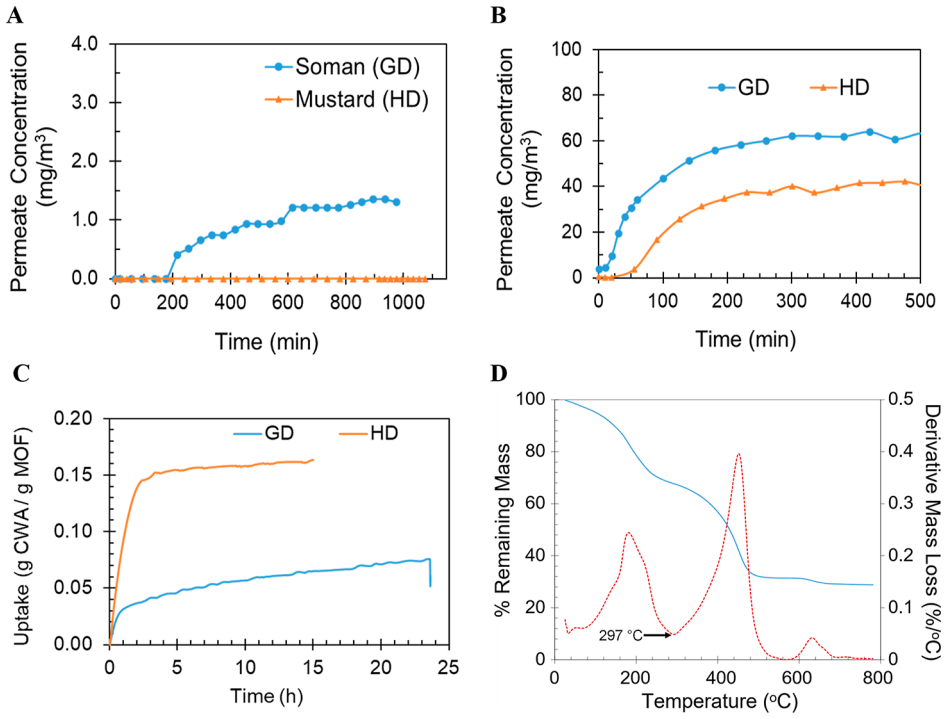

Figure 3. Permeation tests of nerve agent soman (GD) and mustard gas (HD) in cross flow, their MOF sorption behaviors and TGA of the MOF. (A) Individual permeation result through the one layer of GO-membrane (90 mm) stacked on one layer of the MOF-filled ePTFE membrane [(wt of MOF/wt of MOF-filled membrane) = 45%] for 300 mg/m^3 soman (GD) and mustard gas (HD) containing gas streams. (B) Individual agent permeation results through only the MOF layer of the multilayer structure used for (A). (C) HD and GD adsorption capacity measurements of the MOF. (D) TGA data for UiO-66-NH_2.

the pores by exchange with the outside solution containing the reactants. Such a process may not guarantee inside the membrane pores the level of reactants concentration present outside. Here, we bypassed the solvent exchange process and introduced the reactants-containing 80% DMF−20% methanol solution directly into the ePTFE membrane pores by applying vacuum on the other side of the membrane. A higher level of synthesis of MOFs distributed throughout the membrane pores via repeating such a process resulted in a significantly higher breakthrough time of 210 min; this contributed considerably to a long ammonia breakthrough time of 2790 min. This blocking behavior was found to be unaffected by 50% RH. An ePTFE membrane filled with MOF by the earlier method[21] was exposed to 100 ppmv NH_3-containing N_2 gas having 50% RH; the breakthrough time was quite close to that for a dry NH_3-containing N_2 gas.[21] An experiment using a multilayer GO-MOF membrane with the same humidified feed gas blocked NH_3 for more than 6 h when the experiment was stopped.

We will now consider breakthrough studies of two CWAs: mustard gas (HD), $C_4H_8Cl_2S$, bis(2-chloroethyl) sulfide; organophosphorus nerve agent, soman (GD), $C_7H_{16}FO_2P$, 3,3-dimethylbutan-2-yl methylphosphonofluoridate. The blocking of a simulant for HD, namely, 2-CEES, was studied earlier in separate investigations by small samples of the GO membrane[22] as well as by the earlier generation of the UiO-66-NH_2 MOF-filled ePTFE membrane.[21] Figure 3A provides a window into how the multilayer membrane structure blocks the real CWAs instead of the simulant(s). The multilayered membrane having one GO membrane layer on top of a MOF-filled ePTFE membrane layer (wt % of MOF in MOF-filled membrane, 45%), completely blocked HD for 1075 min. The experiment was not extended beyond this time. Previously,[21] we reported a breakthrough concentration of 12 mg/m^3 of 2-CEES (a HD simulant) through a MOF-filled ePTFE membrane (67% MOF filled) on the permeate side per ASTM F 739-12 when exposed in a cross-flow setup of Peske PTF 700 permeation cell with a feed CEES concentration at 300 mg/m^3; 2-CEES was blocked completely for 46.4 min. The individual GO-based membrane completely blocked 2-CEES for only 16 min[22] but limited the plateau concentration of CEES to a very low value of ∼0.25 mg/m^3 for a long period of time. Obviously, this very low level of continuous leakage from the top GO layer was highly useful for the bottom MOF-filled layer to adsorb for an extended time.

The time for complete blockage of GD by the multilayer membrane was on the other hand 176 min (Figure 3A). The breakthrough concentration for GD appears to be a low value 1.2 mg/m^3 under the same test condition and method used for HD. The agent transport data for the multilayer structure illustrating the behavior of Figure 3A are provided in Tables S3 and S4. The individual adsorption-breakthrough behaviors of the MOF-filled bottom membrane layer only for both HD and GD are illustrated in Figure 3B. It appears that HD is almost totally blocked for ∼20 min; the breakthrough concentration value is ∼42 mg/m^3. However, GD does not appear to be totally blocked by this MOF for much time. We need to explore other MOFs possessing superior sorption capabilities for a wider range of CWAs. The breakthrough value for GD is ∼62 mg/m^3. The higher breakthrough value for GD is due to a higher feed agent concentration of ∼375 mg/m^3. The agent transport data for the MOF layer only are available in Tables S5 and S6. The process of MOF synthesis in membrane pores is illustrated in Figures S5 and S6.

https://doi.org/10.1021/acsami.2c07989
ACS Appl. Mater. Interfaces 2022, 14, 31321−31331

The difference in permeation behavior between GD and HD in the MOF layer can be explained by the underlying properties of the MOF itself. The adsorption properties of the MOF were assessed using a Cahn microbalance, where the GD and HD uptake (Figure 3C) were determined to be ∼0.07 and 0.16 g agent per g of MOF, respectively (the setup is shown in Figure S7). Of particular note is the relatively fast uptake of HD, which reaches its approximate equilibrium capacity in ∼2 h, in comparison to GD, which never reaches its full capacity after ∼24 h. This diffusional inhibition is consistent with the MOF having a low fraction of defects. In such a case, the diffusion of GD into the pore structure is inhibited relative to the less sterically hindered HD. Indeed, the MOF surface area (∼984 m^2/g; Table S7) is indicative of low defects. Furthermore, thermogravimetric analysis (TGA) using the method developed by Lillerud and co-workers[38] and shown in Figure 3D led to the conclusion that the MOF had ∼0.02 missing linkers per node, thus supporting the diffusion inhibition toward GD. The temperature plateau at 297 °C was used to calculate the number of defects in the MOF.

Regarding competitive adsorption of moisture with other analytes in the MOF, experiments[39] show that when amine-unfunctionalized UiO-66 type MOF is exposed to 75% humidity for 100 days, the nitrogen-accessible BET surface area remains unchanged. Furthermore, "as long as the RH remains below the condensation step (pore filling), water can safely coexist within the MOF and with other analytes in the pore".[39] Our results for NH_3-containing N_2 stream at 50% RH mentioned earlier support this conclusion.

Figure 4 focuses primarily on the scanning electron microscopy (SEM) of the cross section of the ePTFE membranes where MOF nanocrystals were developed solvothermally inside the interfibrillar space of the ePTFE membrane located below the GO laminate membrane; we also look at the cross section of the GO laminate membrane. The SEM image of Figure 4A illustrates the dense growth of nanocrystals of MOF UiO-66-NH_2 inside and around the fibrillar structure of the ePTFE membrane. This growth was achieved by synthesis carried out three times (Figures S5 and S6) on the same piece of membrane with additional crystal growth taking place each time after the first synthesis step. The crystals (a few identified by red circles) appear to have dimensions of ∼100−200 nm. Figure 4B shows the original SEM from whose marked top left-hand section, material was taken to develop Figure 4A. Figure 4C illustrates the fibrillar structure of the virgin 0.4 μm pore size ePTFE membrane inside whose structural openings MOF crystals were synthesized.

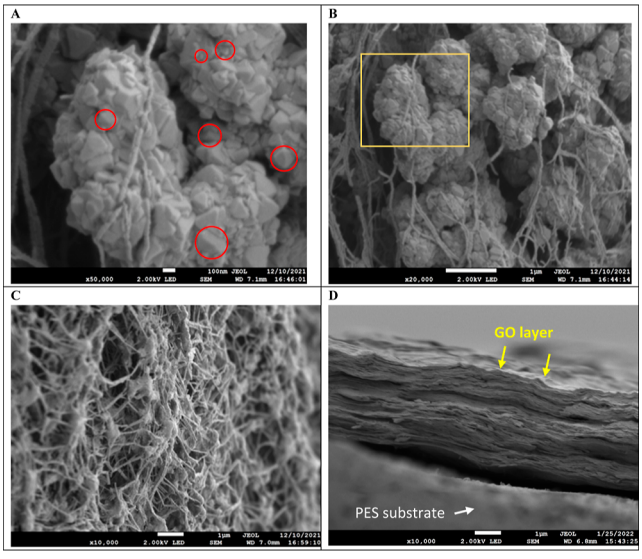

Figure 4. Membrane cross-sectional SEM images for MOF nanocrystals in the ePTFE membrane interfibrillar space and SEM image showing GO laminate membrane thickness. (A) SEM of MOF nanocrystals in the openings/pores of the ePTFE membrane. (B) SEM image shows a profusion of MOF nanocrystal aggregates in ePTFE membrane openings/pores. (C) SEM image of the ePTFE membrane showing its microfibrillar structure. (D) SEM image of the cross section of the GO layer deposited on the PES substrate; GO layer thickness is ∼3 μm (32 mg of GO used with large size PES substrate membrane).

The BET adsorption−desorption behavior and the pore size distribution of the MOF are provided in Figure S8; the corresponding surface areas are provided in Table S7. Around 3μm+ thickness of the laminated GO layer is visible in the SEM image of Figure 4D. The gap between the PES substrate and the bottom surface of the GO layer on top developed during sample preparation at a low temperature. Additional SEM images of the GO layer at 50,000× magnification and the overall GO-PES support layer at a low 500× magnification have been provided in Figure S9.

Figure 5 presents the results of characterizations of the material structures employed in the two individual layers of the multilayer membrane via X-ray diffraction (XRD) and Fourier-transform infrared (FTIR) spectroscopy. The XRD patterns of the GO membrane (without PU coating) and the PES support membrane for both larger and smaller sizes are illustrated in Figure 5A. For the larger size membranes prepared using 32 mg GO, *d*-spacing calculation for the GO laminate based on the first peak located at 9.7° (2θ) is 9.1 Å. There is another smaller peak at 17.7° corresponding to a *d*-spacing of 5 Å. For the 8 mg based smaller size GO-membrane, the peak at 10.0° (2θ) leads to a *d*-spacing of 8.8 Å. There is another peak at 18.2° leading to a *d*-spacing of 4.9 Å. Because the 32 mg amount reflects a proportionate increase from 8 mg due to a larger size porous membrane substrate, we do not expect much variation between the 32 and 8 mg membranes in terms of the XRD pattern. The substrate PES shows a broad peak around 18° as well which is also appearing in the patterns for the GO laminates.

The XRD patterns of the MOF-filled ePTFE membrane illustrated in Figure 5B show two peaks at 2θ values of 7.6 and 8.73 which yield *d*-spacings of 11.6 and 10.1 Å, respectively. These peaks of the MOF, UiO-66-NH_2, have been identified often in literature.[28,29] Figure 5C shows the FTIR spectra of a virgin ePTFE membrane employed to support MOF nanocrystals in the interfibrillar space of an ePTFE membrane along with those of a membrane supporting the MOF nanocrystals. The difference between the two matches clearly with the spectra shown also of the solvothermally synthesized MOF crystals investigated earlier.[21]

In this multilayered structure of a GO laminate-based membrane at the top exposed to the toxic gas mixture and backed up by a porous membrane-supported MOF, UiO-66-NH_2, forming a nano-packed bed at the bottom/permeate side, the top layer acts as a highly water vapor selective membrane drastically reducing the permeation rate of toxic vapors and gases having larger kinetic diameters. The bottom layer acts as

https://doi.org/10.1021/acsami.2c07989
ACS Appl. Mater. Interfaces 2022, 14, 31321−31331

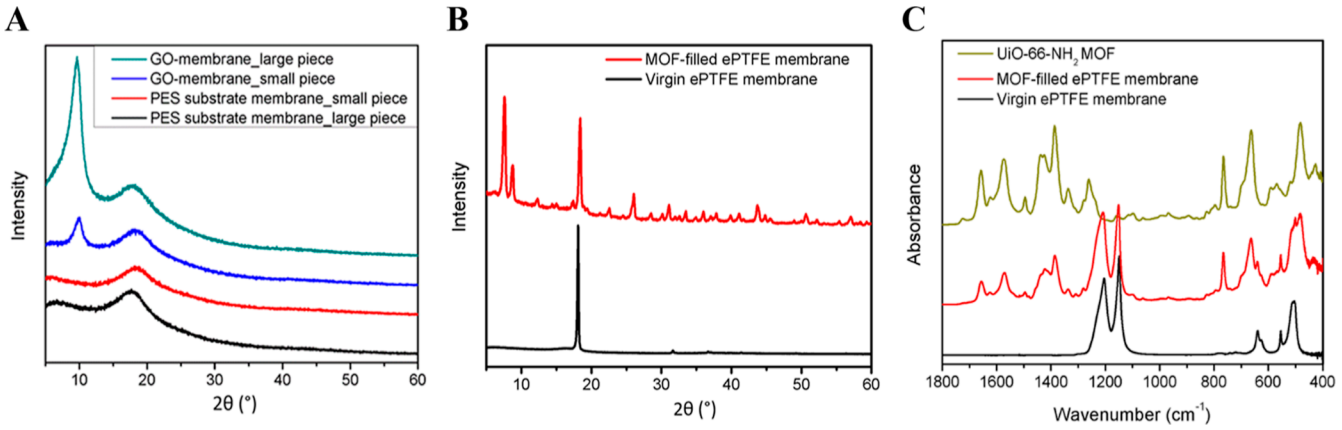

Figure 5. PXRD scans and FTIR spectra of individual components of the multilayer GO-MOF structure. (A) XRD scans of a 32 mg GO-based membrane on a PES substrate (large piece, diameter ~8 cm), an 8 mg GO-based membrane on a PES substrate (small piece, diameter ~4 cm), and the corresponding PES substrate membranes. (B) XRD scans of the UiO-66-NH_2 MOF-filled ePTFE membrane [(MOF/MOF-filled membrane) = 45%, w/w] and virgin ePTFE membrane. (C) FTIR absorption spectra in 1800−400 cm^{-1} range of the following: UiO-66-NH_2 MOF; UiO-66-NH_2 MOF-filled ePTFE membrane; and virgin ePTFE membrane.

a highly moisture permeable nano-packed bed with a high sorption capacity to drastically enhance the time needed for the low level of toxic vapors/gases leaking through the top layer to show up at the other end of the structure. Whereas there are other multilayer structures using GO for mainly mechanical/support perspectives,[22,24] here the two layers have two altogether separate functions from CWA sorption/transport considerations. It is to be recognized also that multilayer structures are frequently used in practice for protective clothings.[5]

CONCLUSIONS

It is useful to emphasize the barrier performances of the multilayer structure for four toxic penetrants. The barrier blocked NH_3, HD, GD, and a sarin simulant, DMMP, completely for 2750, 1075, 176 min, and 7 days, respectively. Our experiments with a top laminated GO layer supported at the bottom by a layer of nanocrystals of a suitable MOF adsorbent in generally sub-micrometer interfibrillar space of a support membrane establish the concept of a highly moisture-permeable barrier that can block toxic vapors, CWAs, and so forth for an extended period. It is highly unlikely that one can have a single membrane or barrier such that it is moisture permeable and yet blocks other toxic gases/vapors for an extended period of time. It is not enough to develop 98−99%+ rejection of toxic gases and vapors in personal protection equipment which some of the more interesting approaches such as a GO laminate-based membrane[22] or a collapsible polymer at the mouth of a CNT[20] were achieving. Complete shut-out is needed for an extended time. Therefore, such membranes/barriers need to be serially reinforced with an adsorbent layer that is highly efficient via porous membrane supported MOF nanocrystals. Correspondingly, other barriers[20] may be used at the top instead of a GO[22] layer and achieve the purpose of a successful barrier membrane. A challenge that remains unanswered is the availability of a barrier permeable to a specific vapor species and completely blocks other species regardless of their type. An additional challenge involves the elimination of the porous PES membrane which supports the laminated GO layer and have the latter supported by the porous membrane layer housing the MOF nanocrystals.

MATERIALS AND EXPERIMENTAL METHODS

Membrane Supports. Hydrophobic expanded polytetrafluoroethylene (ePTFE) membrane (GMM-404: pore size, 0.45 μm; porosity, 80%; thickness, 79 μm; large flat sheet provided; W.L. Gore, Elkton, MD) was used to support MOF nanocrystals. Asymmetric poly (ether sulfone) (PES) membrane (skin side pore size, 0.03 μm; diameter, 47 and 90 mm; thickness, 110−150 μm; Sterlitech, Kent, WA) was employed as the support/substrate of laminated GO layers because its benzene rings can develop noncovalent $\pi-\pi$ interactions with graphene.[30] In a few experiments, a microporous polyether-etherketone (PEEK) membrane (200 nm pore size; diameter, 47 mm; thickness, 20−30 nm) (Sterlitech) was the support.

Materials. The GO flake dimensions were 300−800 nm with a thickness of 0.7−1.2 nm. These single-layer GO flakes were made by modified Hummers' method and obtained from Cheap Tubes (Grafton, VT, OH).

Chemicals. Dimethyl formamide (DMF) (Fisher Chemical, 99.9%), methanol (EMDMillipore, ≥99.8%), zirconium (IV) chloride (Alfa Aesar, >99.5%), and 2-aminoterephthalic acid (H_2BDCNH_2, Acros Organics, 99%) were used for UiO-66-NH_2 MOF synthesis. DMMP (97%), ethylenediamine (EDA) [puriss. p.a., absolute, ≥99.5% (GC)], sodium dodecyl sulfate (SDS) (ACS reagent, ≥99.0%) were bought from Sigma-Aldrich. PU spray was obtained from Minwax (Minwax fast-drying PU semi-gloss oil-based PU: Minwax, Upper Saddle River, NJ). Gas cylinders of He, N_2, 50-50 ethane-ethylene, and CO_2 were from Airgas (Piscataway, NJ). CEES was obtained from Millipore Sigma (97%). *O*-Pinacolyl methylphosphonofluoridate (aka soman, GD, purity 95 ± 1.5%) and bis(2-chloroethyl) sulfide (aka distilled mustard, HD, purity 98.7 ± 0.2%) were obtained at CBC under the chemical agent standard analytical reference Material (CASARM) quality assurance plan.

Preparation of GO Flake-Based Membrane. Six steps, namely, GO suspension preparation, EDA addition, vacuum filtration, physical compression, heat treatment, and PU coating, were implemented to prepare the GO flake-based membranes (see Figure S4). Membranes were prepared in two sizes based on the dimension of the PES support membrane, 47 and 90 mm. The amount of chemicals/materials used varied with the support membrane size. For 90 mm membrane, 32 mg of GO powder was added to 100 mL of deionized (DI) water; 20 mg of SDS was added as dispersant. The diameter of the GO layer deposited on the support membrane is 70 mm. Ultrasonication was used until a clear dispersion was obtained. Then, 10 mL of EDA was added to 100 mL of cold deionized water, and then, more cold water was added to lower the temperature of the solution (two such EDA solution batches were prepared). The reason for keeping the solution cold was to prevent an observed increase in

https://doi.org/10.1021/acsami.2c07989
ACS Appl. Mater. Interfaces 2022, 14, 31321−31331

viscosity due to the potential lowering of the critical micelle concentration of SDS and the corresponding micellization in the presence of amines. The diamine solution was slowly mixed with the GO dispersion with stirring. For 47 mm support membrane, the values of the corresponding quantities are as follows: 8 mg of GO powder, 16 mg of SDS, 100 mL of DI water, and 6 mL of EDA. The diameter of the GO layer deposited on the support membrane is 38 mm.

Then, the substrate polyethersulfone membrane was placed on the vacuum filter holder (47 mm: 80068-654, fritted support assembly, VWR, PA; 90 mm: Z290424, Sigma-Aldrich vacuum filtration assembly) and fixed. Next, suction filtration was carried out to remove all of the water and SDS (wash several times with the second EDA solution with the same concentration in case EDA might be washed away during this process, until no foam can be observed in the exhaust pipe); this usually took 2−3 days. Next, the membrane was taken out and slowly dried in an oven in N_2 atmosphere at 40 °C. The membrane was subjected next to physical compression using a tableting machine (model 3853-0, Carver Inc., Wabash, IN) for 2 min. The membrane was put back into the oven in N_2 atmosphere at 80 °C for an hour to create crosslinking with the amine between various functional groups sticking out of the edges of GO flakes. At the end, a 2 μm thick PU coating on top of the GO membrane was developed via spray coating. An hour gap was provided after coating each time with a total of three coats. Next, the membrane was dried slowly for 48 h before testing. Such membranes were designated PES−EDA−GO−PU. The PU coated side faces the feed gas/vapor during experimental permeation studies.

MOF Synthesis in the ePTFE Membrane via Infiltration under Pressure. Solvothermal synthesis of the MOF, UiO-66-NH_2, employs the reaction of 40 mmol 2-aminoterephthalic acid in 80 g of DMF with 40 mmol $ZrCl_4$ in 20 g of methanol as the appropriate solvent mixture and incorporated in membrane pores. The multistep process resulting in the MOF-filled membrane is illustrated in Figure S5. SDS powder was added to make the mixed solution contain 5 mM SDS. The mixed reactants solution was stirred with a magnetic stirrer for 15 min and sonicated for 15 min by an ultrasonic processor (operating at an amplitude of 80% and pulsed mode: 15 s "on" and 5 s "off"; model #: EW-04714, Cole Parmer, Vernon Hills, IL). The membrane infiltration method can be implemented vis-à-vis pressure assistance in two ways: by pulling a vacuum or by applying pressurized solution over the porous membrane. Here, we describe the vacuum-assisted method due to the larger size of the samples needed as shown in Figure S5; a photo of this part is shown Figure S6.

Virgin microporous hydrophobic ePTFE membrane (GMM404, W. L. Gore) placed in the filtration cell was wetted by pure methanol first. The mixed reactant-containing solution [40 mmol 2-amino-terephthalic acid and 40 mmol $ZrCl_4$ dissolved in 100 g of DMF−methanol mixture (80% DMF, w/w)] (which was also a 5 mM solution of SDS) was introduced into the pores of ePTFE membrane via negative pressure (∼−10 psig) by pulling a vacuum, as shown in Figure S6. The membrane and the remaining solution were transferred into a Teflon-lined sealed vessel. The vessel was put into an oven at 120 °C for 18 h. After the reaction is over, the membrane was washed with methanol, dried at 50 °C for 4 days under vacuum, and weighed to determine the amount of MOF in the membrane. Often the membrane went through 2−3 cycles to enhance the amount of crystals in membrane pores. For such a case, the MOF-filled membrane from the first synthesis cycle was put into freshly prepared mixed reactant-containing solution [40 mmol 2-amino-terephthalic acid and 40 mmol $ZrCl_4$ dissolved in 100 g of DMF−methanol mixture (80% DMF, w/w); has 5 mM SDS]. The same thermal synthesis process was followed after fully soaking. A digital orbital shaker (model SK-O180-Pro, SCILOGEX) was used during the soaking process. One more repeat cycle was applied in the preparation for an even higher MOF loading of the MOF-filled membrane. Then, the membrane was washed with methanol, dried at 50 °C for 4 days under vacuum, and weighed to determine the amount of MOF in the membrane. To be noted here is that during each solvothermal synthesis step, MOF crystals were also synthesized outside the membrane in the solution containing the reactants. Such MOF crystals were also characterized.

Characterization of Various Membranes and MOF. Powder XRD (PXRD) patterns of the MOF in the membrane pores and the GO membrane were obtained in an Empyrean multipurpose PXRD with PIXcel1D detector (serial no. 202627, PANalytical). PXRD patterns of all MOF samples were scanned by Cu Kα radiation (λ = 1.54 Å, 40 mA, 45 kV) from 2 to 60° of 2θ, step size = 0.0260°(2θ), and scan step time = 99.176 s. The corresponding details for the GO membrane are as follows: 5 to 60° of 2θ, step size = 0.0260° (2θ) to provide guidance on different values of the interlayer gaps. A closed sample box was used to store samples prior to testing. An Agilent Cary 670 (Agilent, Santa Clara, CA) Fourier transform infrared (FTIR) spectrometer was employed for FTIR spectra of samples of both the GO and MOF samples; 32 scans were taken for each sample over 6000−400 cm^{-1} with a resolution of 4 cm^{-1}. Membrane cross-sectional images were obtained by SEM in field emission-scanning electron microscopy (FE-SEM, model JSM-7900F; JEOL USA, Peabody, MA). The samples were mounted on the SEM stubs by carbon tape and coated with 8 nm of gold by turbomolecular pumped coater (model EMS Q150T ES).

An automated gas sorption analyzer (model #: ASIQM000000-6, Quantachrome Instruments, Boynton Beach, FL) was employed to collect N_2 isotherm curves of samples. Commercial DFT software combined with the instrument operation interface was used to calculate pore size distribution and Brunauer−Emmett−Teller (BET) surface area. Before starting BET measurement, membrane samples were degassed at 70 °C for 48 h and UiO-66-NH_2 MOF samples were degassed at 120 °C for 18 h.

Adsorption capacity was obtained by measuring the uptake of CWA vapor in terms of agent mass adsorbed onto an experimental test sample of fabric or powder at both a fixed temperature and vapor phase concentration in a setup shown in Figure S7. By using the vapor pressure and temperature relationships of HD[40] and GD,[41] high-purity CWA [CASARM HD lot # HD-U-2086-CTF-N was 98.7 ± 0.2 mol percent pure (determined by melting point); CASARM GD lot # GD-U-2277-CTF-N, was 95.3 ± 1.5 weight percent by ^{31}P NMR spectroscopy], and a modified ASTM saturator methodology,[42] the vapor-phase concentration of each agent was selected, precisely generated, diluted in purified dry air, and safely transported to the sorbent sample, all within the confines of an approved fume hood.

The adsorbent sample (3−5 mg) was placed in a small, gold-plated, stainless steel, mesh basket suspended from an arm of the calibrated Cahn (Orion Research Inc., Boston, MA) model D-200 microbalance by a thin wire. The wire and basket were located in the central cavity of the quartz test chamber. An initial drying step allowed for the removal of water from the sorbent. The temperature of the drying step was obtained by resistive heating using nichrome wire located within a series of glass coils within the inner cavity of the test chamber and near the suspended basket. Thermally stable powders were heated at 100 °C for 30 min under a dry air flow rate equal to the total flow rate of the uptake experiment, either 0.5 or 1.0 L per min (LPM). Thermally sensitive fabrics receive moderate heat at 40 °C for 30 to 60 min under a dry air flow rate of either 0.5 or 1.0 LPM.

Starting and final sorbent masses were recorded with the sample at well controlled laboratory ambient temperature under a no flow condition after a 2-minute pause to ensure microbalance stability. During the uptake experiment, the CWA vapor was passed over the adsorbent with mass changes recorded using an in-house LabVIEW (National Instruments) based data acquisition and control system. The agent vapor exited the test chamber and was scrubbed by a carbon filter. Static issues were eliminated using an Americium-241 source in line with basket. The experiment was determined to be complete when there is no observable change in sorbent mass.

Vapor Permeance Measurement by Upright Cup Method. This method uses a cup-like test cell for holding a volatile sample liquid (Figure S1). The cup is filled with a liquid to be tested (e.g., water, DMMP) and covered with the multilayer membrane barrier to be tested. The GO side of the membrane faced the test liquid; the back side of the MOF filled membrane is exposed to the environment

https://doi.org/10.1021/acsami.2c07989
ACS Appl. Mater. Interfaces 2022, 14, 31321−31331

of a desiccator in which the assembled test cell is located. For water as the test liquid, the RH in this cell is very high (~90% RH) and water vapor (e.g.) migrates across the membrane into the very dry permeate side (~1−5% RH) in the desiccator. The experiment was carried out under such a condition for 7 or more days; the weight loss of the entire setup was measured once every day over the whole week. The test cell cup was made of PVC (the membrane area in the cell was 2.85×10^{-4} m^2). In some experiments, to avoid sorption of the chemical by the PVC material, a thin metallic foil was used to shield the polymer material forming the cup. The membrane area in the cell for these experiments was smaller, 1.77×10^{-4} m^2; temperature was 25 °C.

Water Vapor Permeance Measurement in DMPC. The diameter of the circular composite membrane in the DMPC[31] is 47 mm. The effective membrane area in the cell was 7.07×10^{-4} m^2. Temperature was 25 °C. The RH in the feed side of the cell was very high (~90% RH). Water vapor migrated across the membrane into the dry permeate side (~1−5% RH). Relative humidities of both streams were measured by four RH transducers (HMP76, Vaisala, Woburn, MA). The pressure difference maintained between the two inlet locations (feed inlet and sweep inlet) was less than ~0.1 inch of water during moisture permeation measurement. Certain flow rates of gases were employed both in the feed side (pure N_2) and sweep side (pure He). To determine the permeance of moisture and N_2, the gas flow rates on both sides were maintained at the same value; these values were 20, 50, 100, 200, and 500 cm^3/min. The pressures were essentially atmospheric. A gas chromatograph (GC) (GC-2014, SHIMADZU) was used with a thermal conductivity detector (TCD); the column used for N_2 was as follows: fused silica capillary column (30 m × 0.53 mm; Supelco Analytical). The conditions used were as follows: carrier gas temperature, 200 °C; column temperature, 180 °C; and detector temperature 230 °C.

Experiments for Ammonia Breakthrough Studies. A dry nitrogen gas stream containing 100 ppmv NH_3 was introduced to the feed side of the DMPC at 10 cm^3/min flow rate from a gas cylinder having this N_2 calibration gas mixture (Gasco, Oldsmar, FL). On the other side of the cell, ultrahigh purity N_2 gas (UHP NI 300, Airgas, Oakland, NJ) was introduced at the same flow rate (Figure S10). The very low level of ammonia in the counter-currently flowing stream was analyzed by a CMS analyzer (Draeger, Telford, PA) with ammonia CMS chips (0.2−5 ppm, model 6406550, 2−50 ppm, model 6406130, 10−150 ppm, model 6406020, Draeger, Telford, PA).

Testing of Breakthrough of CWAs. The testing of CWAs, HD, GD was carried out according to ASTM F 739-12. A schematic of the 1inch diameter Pesce PTF 700 permeation test cell used is shown in Figure S11. A sample membrane was cut out to the required dimension of the cell. The permeation area is 5.02 cm^2. Dry air was introduced to both sides of the cell in a countercurrent fashion at 300 cm^3/min. Into the air entering the challenge side of the cell, the CWA or its simulant was introduced from a saturator cell at a rate sufficient to develop a concentration of 300 mg/m^3 concentration. When the CWA/simulant breaks through completely at its feed concentration level through the membrane into the collection chamber, its concentration level measured from the air stream exiting the collection chamber is going to be considerably lower due to dilution.

■ ASSOCIATED CONTENT

Supporting Information

The Supporting Information is available free of charge at https://pubs.acs.org/doi/10.1021/acsami.2c07989.

Upright cup method and test cell for vapor permeance determination; upright cup method results for water vapor and DMMP for GO-MOF composite membrane for 7 days; transmission rates of moisture in upright cup method for GO laminate and other membranes; DMPC for gas (vapor) permeation studies; species permeances through multilayered GO-MOF membrane for several gases/vapors in a permeation apparatus having a DMPC; steps followed for preparing laminated GO membrane: PES−EDA−GO−PU; nerve agent soman (GD) permeation tests in cross flow for multilayered membrane; sulfur mustard (HD) permeation tests in cross flow for multilayered membrane; nerve agent soman (GD) permeation tests in cross flow over one layer of MOF-filled ePTFE membrane; sulfur mustard (HD) permeation tests in cross flow over one layer of MOF-filled ePTFE membrane; multistep process for obtaining an ePTFE membrane whose pores are filled with in situ synthesized nanocrystals of MOF; photo of the experimental setup for introducing mixed reactant-containing solution into the microporous ePTFE membrane with assistance of vacuum; adsorption measurement setup using Cahn microbalance for CWAs; BET isotherms of virgin ePTFE membrane, ePTFE membrane filled with MOF, UiO-66-NH_2, and only MOF UiO-66-NH_2 and their pore size distributions; BET-based surface area estimates; SEM cross-sectional photo of the GO layer deposited on the PES substrate; schematic for ammonia breakthrough testing using the DMPC; and Pesce PTF 700 permeation cell for ASTM F 739-12 (PDF)

■ AUTHOR INFORMATION

Corresponding Author

Kamalesh K. Sirkar − *Department of Chemical and Materials Engineering, New Jersey Institute of Technology, Newark, New Jersey 07102, United States;* orcid.org/0000-0001-7157-5010; Phone: 973-596-8447; Email: sirkar@njit.edu; Fax: 973-642-4854

Authors

Yufeng Song − *Department of Chemical and Materials Engineering, New Jersey Institute of Technology, Newark, New Jersey 07102, United States*

Cheng Peng − *Materials Science and Engineering, New Jersey Institute of Technology, Newark, New Jersey 07102, United States*

Zafar Iqbal − *Department of Chemistry and Environmental Science, New Jersey Institute of Technology, Newark, New Jersey 07102, United States*

Gregory W. Peterson − *CBR Filtration Branch, R&T Directorate DEVCOM Chemical Biological Center, Aberdeen Proving Ground, Maryland 21010, United States;* orcid.org/0000-0003-3467-5295

John J. Mahle − *CBR Filtration Branch, R&T Directorate DEVCOM Chemical Biological Center, Aberdeen Proving Ground, Maryland 21010, United States*

James H. Buchanan − *CBR Filtration Branch, R&T Directorate DEVCOM Chemical Biological Center, Aberdeen Proving Ground, Maryland 21010, United States*

Complete contact information is available at: https://pubs.acs.org/10.1021/acsami.2c07989

Author Contributions

The manuscript was written through contributions of all authors. All authors have given approval to the final version of the manuscript.

Notes

The authors declare the following competing financial interest(s): A patent application has been filed.

■ ACKNOWLEDGMENTS

The authors gratefully acknowledge support for this research from DTRA contract # HDTRA 1-16-1-0028. This research was carried out in the NSF Industry/University Cooperative Research Center for Membrane Science, Engineering and Technology that has been supported via two NSF Awards IIP1034710 and IIP-1822130. We are grateful to W.L. Gore Inc. for donating GMM-404 membranes of PTFE to our research.

■ REFERENCES

(1) Nagarajan, R.; Zukas, W.; Hatton, T. A.; Lee, S.; *Nanoscience and Nanotechnology for Chemical and Biological Defense*; ACS Symposium Series; American Chemical Society, 2009; Vol. *1016*, p 368.
(2) Romano, J. A., Jr.; Salem, H.; Lukey, B. J.; Lukey, B. J. *Chemical Warfare Agents: Chemistry, Pharmacology, Toxicology, and Therapeutics*; CRC Press, 2007, pp 21−50.
(3) Napadensky, E.; Elabd, Y. A. *Breathability And Selectivity Of Selected Materials For Protective Clothing, No. ARL-TR-3235*; Army Research Lab-Weapons and Materials Research Directorate: Aberdeen Proving Ground MD, 2004.
(4) Wartell, M. A.; Kleinman, M. T.; Huey, B. M.; Duffy, L. M. *Strategies to Protect the Health of Deployed U.S. Forces: Force Protection and Decontamination*; National Academy Press: Washington, D.C., 1999.
(5) Lomax, G. R. Breathable polyurethane membranes for textile and related industries. *J. Mater. Chem.* **2007**, *17*, 2775−2784.
(6) Rother, M.; Barmettler, J.; Reichmuth, A.; Araujo, J. V.; Rytka, C.; Glaied, O.; Pieles, U.; Bruns, N. Self-Sealing and Puncture Resistant Breathable Membranes for Water-Evaporation Applications. *Adv. Mater.* **2015**, *27*, 6620−6624.
(7) *Approval of Respiratory Protective Devices*; Code of Federal Regulations, 1995.report
(8) Peterson, G. W.; DeCoste, J. B.; Fatollahi-Fard, F.; Britt, D. K. Engineering UiO-66-NH_2 for toxic gas removal. *Ind. Eng. Chem. Res.* **2014**, *53*, 701−707.
(9) Jasuja, H.; Peterson, G. W.; Decoste, J. B.; Browe, M. A.; Walton, K. S. Evaluation of MOFs for air purification and air quality control applications: Ammonia removal from air. *Chem. Eng. Sci.* **2015**, *124*, 118−124.
(10) Rieth, A. J.; Dincă, M. Controlled Gas Uptake in Metal-Organic Frameworks with Record Ammonia Sorption. *J. Am. Chem. Soc.* **2018**, *140*, 3461−3466.
(11) Rieth, A. J.; Dincă, M. Programming framework materials for ammonia capture. *ACS Cent. Sci.* **2018**, *4*, 666−667.
(12) Peterson, G. W.; Lu, A. X.; Epps, T. H., III Tuning the Morphology and activity of Electrospun polystyrene/UiO-66-NH_2 metal−organic framework composites to enhance chemical warfare agent removal. *ACS Appl. Mater. Interfaces* **2017**, *9*, 32248−32254.
(13) Eum, K.; Ma, C.; Rownaghi, A.; Jones, C. W.; Nair, S. ZIF-8 Membranes via interfacial microfluidic processing in polymeric hollow fibers: Efficient propylene separation at elevated pressures. *ACS Appl. Mater. Interfaces* **2016**, *8*, 25337−25342.
(14) Zhao, Z.; Ma, X.; Kasik, A.; Li, Z.; Lin, Y. S. Gas separation properties of metal organic framework (MOF-5) membranes. *Ind. Eng. Chem. Res.* **2012**, *52*, 1102−1108.
(15) Lin, Y. Metal organic framework membranes for separation applications. *Curr. Opin. Chem. Eng.* **2015**, *8*, 21−28.
(16) Lin, J. Y. S. Molecular sieves for gas separation. *Science* **2016**, *353*, 121−122.
(17) Kovvali, A. S.; Chen, H.; Sirkar, K. K. Dendrimer membranes: A CO_2-selective molecular gate. *J. Am. Chem. Soc.* **2000**, *122*, 7594−7595.
(18) Peterson, G. W.; Browe, M. A.; Durke, E. M.; Epps, T. H., III Flexible SIS/HKUST-1 Mixed matrix composites as protective barriers against chemical warfare agent simulants. *ACS Appl. Mater. Interfaces* **2018**, *10*, 43080−43087.
(19) Bui, N.; Meshot, E. R.; Kim, S.; Peña, J.; Gibson, P. W.; Wu, K. J.; Fornasiero, F. Ultrabreathable and Protective Membranes with Sub-5 nm Carbon Nanotube Pores. *Adv. Mater.* **2016**, *28*, 5871−5877.
(20) Li, Y.; Chen, C.; Meshot, E. R.; Buchsbaum, S. F.; Herbert, M.; Zhu, R.; Kulikov, O.; McDonald, B.; Bui, N. T. N.; Jue, M. L.; Park, S. J.; Valdez, C. A.; Hok, S.; He, Q.; Doona, C. J.; Wu, K. J.; Swager, T. M.; Fornasiero, F. Autonomously responsive membranes for chemical warfare protection. *Adv. Funct. Mater.* **2020**, *30*, 2000258.
(21) Song, Y.; Chau, J.; Sirkar, K. K.; Peterson, G. W.; Beuscher, U. Membrane-supported metal organic framework based nanopacked bed for protection against toxic vapors and gases. *Sep. Purif. Technol.* **2020**, *251*, 117406.
(22) Peng, C.; Iqbal, Z.; Sirkar, K. K.; Peterson, G. W. Graphene Oxide-Based Membrane as a Protective Barrier against Toxic Vapors and Gases. *ACS Appl. Mater. Interfaces* **2020**, *12*, 11094−11103.
(23) Nair, R. R.; Wu, H. A.; Jayaram, P. N.; Grigorieva, I. V.; Geim, A. K. Unimpeded Permeation of Water Through Helium-Leak-Tight Graphene-Based Membranes. *Science* **2012**, *335*, 442−444.
(24) Spitz Steinberg, R.; Cruz, M.; Mahfouz, N. G. A.; Qiu, Y.; Hurt, R. H. Breathable Vapor Toxicant Barriers Based on Multilayer Graphene Oxide. *ACS Nano* **2017**, *11*, 5670−5679.
(25) Chen, P.-Y.; Zhang, M.; Liu, M.; Wong, I. Y.; Hurt, R. H. Ultrastretchable graphene-based molecular barriers for chemical protection, detection, and actuation. *ACS Nano* **2018**, *12*, 234−244.
(26) Petukhov, D. I.; Chernova, E. A.; Kapitanova, O. O.; Boytsova, O. V.; Valeev, R. G.; Chumakov, A. P.; Konovalov, O. V.; Eliseev, A. A. Thin graphene oxide membranes for gas dehumidification. *J. Membr. Sci.* **2019**, *577*, 184−194.
(27) Eliseev, A. A.; Poyarkov, A. A.; Chernova, E. A.; Eliseev, A. A.; Chumakov, A. P.; Konovalov, O. V.; Petukhov, D. I. Operando study of water vapor transport through ultra-thin graphene oxide membranes. *2D Mater.* **2019**, *6*, 035039.
(28) Cavka, J. H.; Jakobsen, S.; Olsbye, U.; Guillou, N.; Lambert, C.; Bordiga, S.; Lillerud, K. P. A new zirconium inorganic building brick forming metal organic frameworks with exceptional stability. *J. Am. Chem. Soc.* **2008**, *130*, 13850−13851.
(29) Kandiah, M.; Nilsen, M. H.; Usseglio, S.; Jakobsen, S.; Olsbye, U.; Tilset, M.; Larabi, C.; Quadrelli, E. A.; Bonino, F.; Lillerud, K. P. Synthesis and stability of tagged UiO-66 Zr-MOFs. *Chem. Mater.* **2010**, *22*, 6632−6640.
(30) Kuila, T.; Mishra, A. K.; Khanra, P.; Kim, N. H.; Uddin, M. E.; Lee, J. H. Facile Method for the Preparation of Water Dispersible Graphene using Sulfonated Poly(ether-ether-ketone) and Its Application as Energy Storage Materials. *Langmuir* **2012**, *28*, 9825−9833.
(31) Gibson, P. W.; Kendrick, C. E.; Rivin, D.; Charmchi, M. An automated dynamic water vapor permeation test method. *Performance of Protective Clothing*; ASTM International, 1997, *6*, pp. 93−107.
(32) Sirkar, K. K. Membranes, Phase Interfaces, and Separations: Novel Techniques and Membranes-An Overview. *Ind. Eng. Chem. Res.* **2008**, *47*, 5250−5266.
(33) Barrer, R. M. Diffusion and permeation in heterogeneous media. In *Diffusion in Polymers*; Crank, J., Park, G. S., Eds.; Academic Press: New York, NY, 1968. Chapter 6, Figure 5b
(34) Sainath, K.; Modi, A.; Bellare, J. CO_2/CH_4 mixed gas separation using graphene oxide nanosheets embedded hollow fiber membranes: Evaluating effect of filler concentration on performance. *Chem. Eng. J. Adv.* **2021**, *5*, 100074.
(35) Zhao, Y.; Zhou, C.; Kong, C.; Chen, L. Ultrathin reduced graphene oxide/organosilica hybrid membrane for gas separation. *J. Autism Child. Schizophr.* **2021**, *1*, 328−335.
(36) Jin, X.; Foller, T.; Wen, X.; Ghasemian, M. B.; Wang, F.; Zhang, M.; Bustamante, H.; Sahajwalla, V.; Kumar, P.; Kim, H.; Lee, G. H.; Kalantar-Zadeh, K.; Joshi, R. Effective separation of CO_2 using metal-incorporated rGO Membranes. *Adv. Mater.* **2020**, *32*, 1907580.
(37) Wang, H.; Zheng, J.; Zhao, J.; Jin, W. Designing GO channels with high selectivity for CO_2/N_2 separation via incorporating metal ions. *Chem.−Asian J.* **2021**, *16*, 3141−3150.

https://doi.org/10.1021/acsami.2c07989
ACS Appl. Mater. Interfaces 2022, 14, 31321−31331

(38) Shearer, G. C.; Chavan, S.; Bordiga, S.; Svelle, S.; Olsbye, U.; Lillerud, K. P. Defect Engineering: Tuning the Porosity and Composition of the Metal-Organic Framework UiO-66 via Modulated Synthesis. *Chem. Mater.* **2016**, *28*, 3749−3761.
(39) Lawrence, M. C.; Katz, M. J. Analysis of the Water Adsorption Isotherms in UiO-Based Metal-Organic Frameworks. *J. Phys. Chem. C* **2022**, *126*, 1107−1114.
(40) Buchanan, J. H.; Buettner, L. C.; Tevault, D. E. Vapor pressure of solid bis(2-chloroethyl) sulfide. *J. Chem. Eng. Data* **2006**, *51*, 1331−1334.
(41) Balboa, A.; Buchanan, J. H.; Buettner, L. C.; Sewell, T.; Tevault, D. E. *Vapor Pressure Of GD; Report ECBC-TR-575*; Edgewood Chemical Biological Center: Aberdeen Proving Ground: MD, 2007.
(42) Buchanan, J. H.; Sumpter, K. B.; Abercrombie, P. L.; Tevault, D. E. *Vapor Pressure Of GB; Report ECBC-TR-686*; Edgewood Chemical Biological Center: Aberdeen Proving Ground: MD, 2009.

https://doi.org/10.1021/acsami.2c07989
ACS Appl. Mater. Interfaces 2022, 14, 31321−31331